NUMERICAL SIMULATIONS OF GAP FLOW ABOVE ROTATING DISK

FILIP WASILCZUK[1,2], PAWEŁ FLASZYŃSKI[1]
AND PIOTR DOERFFER[1]

[1]*Institute of Fluid-Flow Machinery, Polish Academy of Sciences*
Fiszera 14, 80-952 Gdansk, Poland

[2]*Interdepartmental PhD Studies at the Gdansk University of Technology*
Narutowicza 11/12 80–233 Gdansk, Poland

(received: 5 January 2015; revised: 6 February 2015;
accepted: 10 February 2015; published online: 20 March 2015)

Abstract: A rotating disk can be considered a basic configuration for the investigations of the impact of various conditions on the flow through the clearance between the shrouded turbine blade and the casing. Numerical calculations using Fine/Turbo Numeca were conducted to examine the influence of the rotational velocity and the pressure difference across the disk on the flow conditions, especially the mass flow through the clearance. The results were validated using the experimental data. Moreover, the flow field was investigated to reveal the vortices induced in the flow. The calculations showed a significant drop of the mass flow with a rise of the rotation velocity. Additionally, the vortex created upstream of the disk at higher rotation velocities was observed. The phenomenon of separation at the edge of the disk was investigated.

Keywords: computational fluid dynamics, internal flow, flow control

Notation

m – mass flow rate,
μ – mass flow rate coefficient,
S – area of the clearance between the disk and the casing
ρ – fluid density
Δp – pressure drop on the disk
u – disk rotation velocity
w – average fluid velocity in the gap assuming isentropic expansion
u/w – rotation velocity to fluid velocity for isentropic expansion ratio
l – vortex length
h – gap height
δ – disk thickness

1. Introduction

The turbine blade tip clearance between the blade and the casing is a significant design feature and it has a strong effect on the turbine performance. Excessive tip clearance influences power losses and decreases efficiency. On the other hand, insufficient tip clearance leads to tip rub and it can be a reason for damage in extreme conditions. Its minimal size depends on the turbine design, however, robustness is the ultimate goal when it is determined. For that reason different measures have to be taken to reduce the flow through the clearance, other than just reducing its size.

The numerical investigations presented in the paper concern the basic configuration, which can be considered as simplification of the clearance in a shrouded turbine cascade. Puzyrewski and Jakubek [1, 2] have proposed an experiment to determine the impact of the plate configuration on the flow rate through the gap between the rotating disk and the casing. Assessment of the impact of various parameters on the mass flow rate in the gap can be investigated at the proposed test rig, modeling the leakage flow over a shrouded turbine stage. The numerical simulations results are compared with experimental data and the validated numerical model is used for further flow structure analysis.

There is a significant difference between a model with a disk and an actual turbine. In the turbine, the flow is generated by the pressure difference upstream and downstream of the passage. The flow goes through the flow passage and the tip gap (leakages), whereas in the model with a disk it flows through the gap, only. The consequences of that difference will be discussed in the paper.

There are several measures that can be taken to reduce the flow through the gap. The passive methods include modification of the tip geometry in unshrouded turbine blades [3, 4] and introducing labyrinth sealing in the shrouded blades [5–8]. Moreover active methods such as the use of cooling holes to change the flow structure [4, 8] or plasma actuators to generate vortices can be used [9].

2. Experiment summary

A rotating disk, driven by a motor, was mounted in a tube. Upstream of the disk, the pressure was controlled and the mass flow was measured with the orifice. The mass flow rate can be calculated according to the formula:

$$m = \mu S \sqrt{2\rho \Delta p} \tag{1}$$

Based on the measured mass flow rate and the pressure drop, the mass flow rate coefficient "μ" can be calculated. The mass flow coefficient is plotted against the "u/w", where: "u" – the disk circumferential velocity at the outer radius, and "w" – the velocity for isentropic expansion. The experiment was carried out for several disk thicknesses, pressure differences and rotational velocities. An example of the mass flow coefficient for different pressure difference for the 7.1 mm disk thickness is shown in Figure 1.

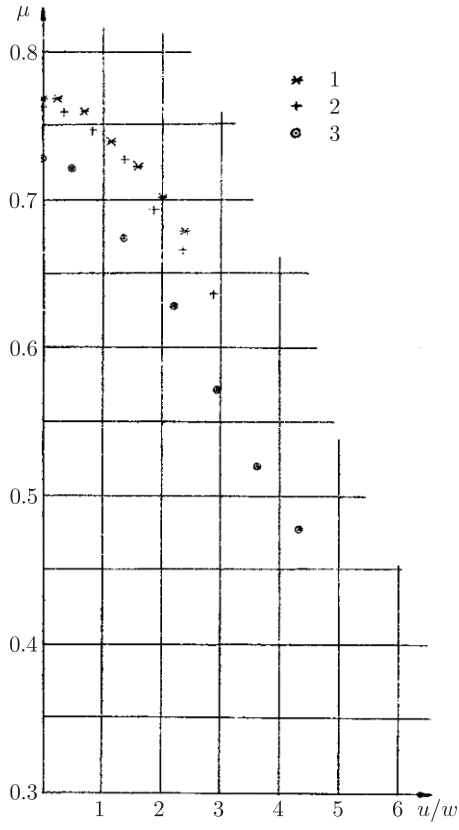

Figure 1. Mass flow coefficient μ vs. u/w ratio.
1 – $\Delta p = 1687\,\text{Pa}$, 2 – $\Delta p = 916\,\text{Pa}$, 3 – $\Delta p = 363\,\text{Pa}$ [1]

The relation between the flow rate coefficient μ and the u/w ratio was established. [1]

$$\mu = 0.829\sqrt{1 - 0.132^2\left(\frac{u}{w}\right) - 0.011\frac{L}{\delta\left(1+0.242\frac{u}{w}\right)}} \tag{2}$$

Moreover the velocity profile upstream of the disk was investigated experimentally [2]. The disk was placed in a transparent pipe, and the smoke generator was used to visualize the flow. The experiment revealed that at higher circumferential velocity a vortex is created upstream of the disk, near the pipe wall.

3. Geometry and numerical model description

The geometry is created according to test section dimensions. Simulations were carried out for the rotating disk with a radius of 75 mm and a thickness of 7.1 mm within a framework of an axisymmetric model. The structured two-dimensional (2D) mesh is shown in Figures 3–4.

The inner diameter of the casing is 76 mm, thus the gap height is 1 mm. The 2D mesh contains 35 666 nodes. In the experiment the rotating disk was

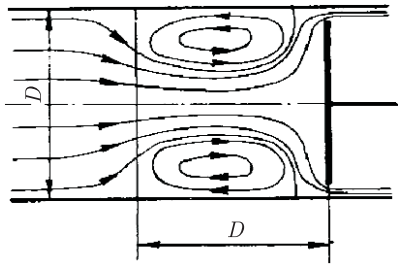

Figure 2. 2D graphic interpretation of flow field upstream of disk based on experiment [2]

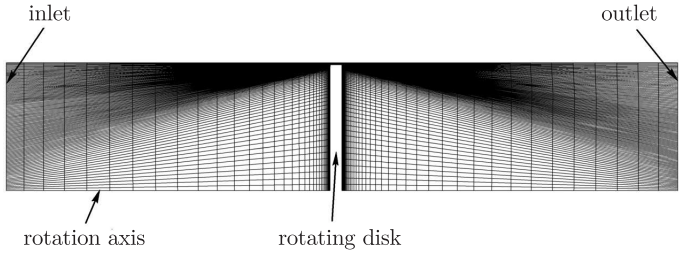

Figure 3. 2D mesh of rotating disk in cylindrical channel

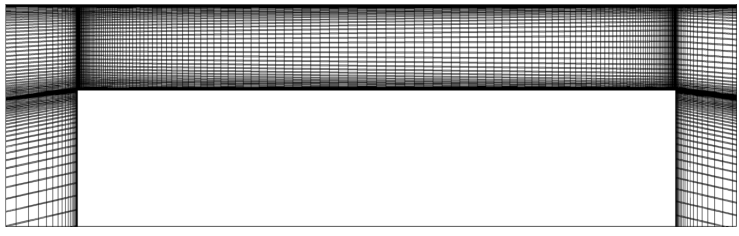

Figure 4. Close up of gap between disk and casing meshed in 2D mesh

connected to the electric motor (located downstream). There is no data available on the shaft diameter and it is assumed that its impact on the flow is negligible, hence, it was not included in the CFD model.

Numerical simulations were carried out with Fine/Turbo Numeca. The investigated flow structure is considered as steady and turbulent. The Spalart-Allmaras [10] turbulence model was used for most of the investigated flow conditions.

Inlet: Appropriate inlet pressure values were set for various Δp are presented in Table 1.

The inlet temperature was set to 293 K.The turbulence viscosity of $0.0001\,\mathrm{m}^2/\mathrm{s}$ was set as the boundary condition for the Spalart-Allmaras [10] model, what corresponds to the turbulent viscosity ratio 10.

Outlet: The constant static pressure at the outlet was set as 99 kPa.

Walls: Solids were set to impermeable, no slip. Moreover, the rotational speed was set at the rotating disk walls.

Table 1. Inlet total pressure values

Δp (Pa)	Total pressure at inlet (Pa)
363	99 363
700	99 700
981	99 981
1300	100 300
1687	100 687
1800	100 800
2000	101 000
2200	101 200

4. Model validation

Firstly, the mesh independence was assessed, which revealed that the obtained results were mesh independent. Moreover, the numerical simulations results were validated by comparison with the aforementioned experimental data obtained by Puzyrewski and Jakubek [1]. In Figure 5, the experimental data together with the numerical results for $\Delta p_1 = 363\,\text{Pa}$, $\Delta p_2 = 981\,\text{Pa}$, $\Delta p_3 = 1687\,\text{Pa}$ are shown. For a higher pressure difference case, the results are in good agreement with experimental data. In the case of $\Delta p = 363\,\text{Pa}$, the mass flow (and therefore the mass flow coefficient) is overpredicted up to 8% in comparison with the experiment. However, the overall trend of the μ to u/w relation is properly predicted.

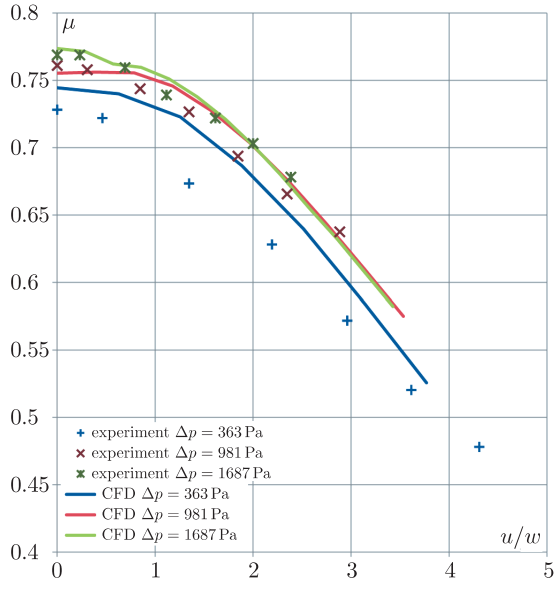

Figure 5. Mass flow coefficient μ vs. u/w ratio – comparison between CFD calculation and experiment

5. Results of numerical simulations

Firstly, the flow significantly accelerates in the gap due to the contraction (Figure 6), so the velocity increases in this zone. The magnitude of the velocity increase depends on the pressure difference. The velocity direction is influenced by the circumferential velocity component near the disk wall, rising with rotational speed.

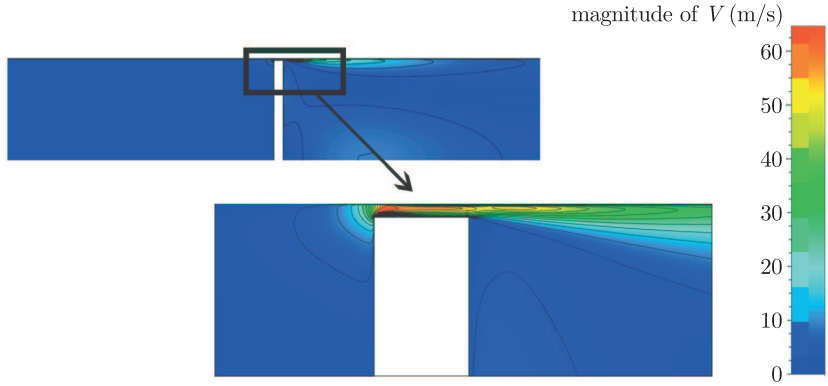

Figure 6. Velocity magnitude in the gap

In Figure 7, the mass flow coefficient μ as a function of u/w for the three investigated pressure differences: 363 Pa, 981 Pa and 1687 Pa is shown. Regardless of the pressure difference the mass flow coefficient decreases with the increasing circumferential velocity. It is caused by the disk rotation. The rotation drives the fluid in the circumferential direction, which is the reason why the streamlines are not parallel to the axial direction. Thus, the fluid has to cover a longer distance in the gap, so the viscous losses are larger. It results in a decreased mass flow. Moreover, looking from the point of view of the inertial reference frame, the fluid is given the velocity component tangent to the disk, what generates centrifugal forces pushing them onto the pipe wall. The mass flow coefficient depends also on the pressure difference.

The mass flow reduction was defined as the difference between the mass flow without rotation and the mass flow with the given rotation, divided by the mass flow with no rotation. Reduction was plotted against the rotational velocity (Figure 8). It can be observed that the impact of the rotational velocity on the mass flow reduction is more significant for lower pressure differences.

An interesting phenomenon occurs upstream of the disk for certain flow parameters. A vortex is created upstream of the gap, near the channel wall. Its existence depends on both the circumferential speed and the pressure difference. For lower pressure differences, the lower rotation velocity is needed for the vortex to be created. Figure 9 shows the streamlines in the region between the inlet (left hand side) and the disk (right hand side). The gap is located in the upper right corner of the figure.

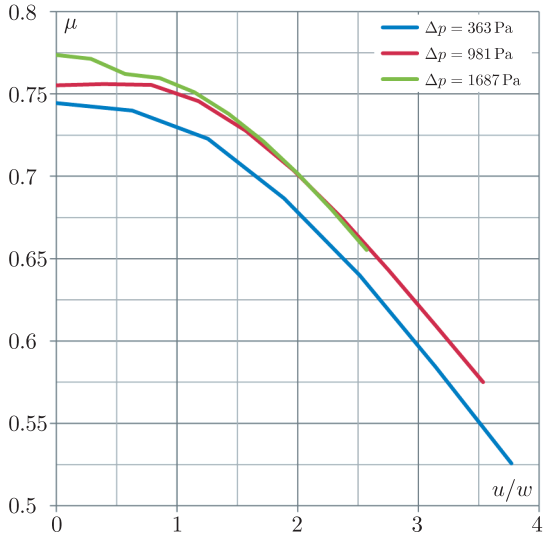

Figure 7. Mass flow coefficient μ vs. u/w ratio

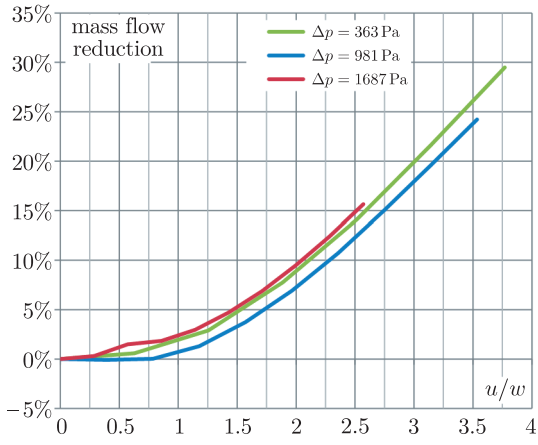

Figure 8. Mass flow reduction with respect to u/w

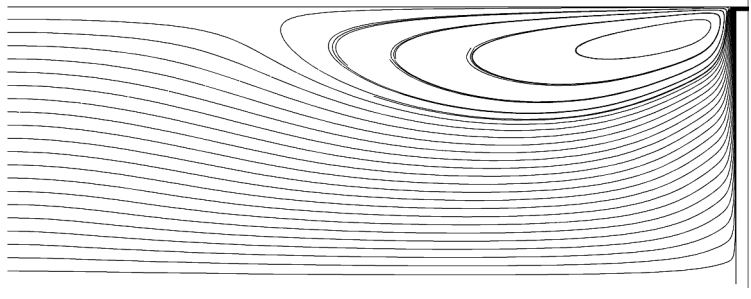

Figure 9. Streamlines upstream of rotating disk for rotational velocity $n = 18\,000$ RPM

Both the experiment and the CFD calculation show that the vortex is created upstream of the disk at higher circumferential velocities. Due to the nature of the experiment and the equipment available at the time when it was conducted, the exact size and shape of the vortex could not be measured. Even though, it could be observed that the phenomenon was escalating when the circumferential velocity rose. It agrees well with the results of the numerical calculations. The disk rotation enforces the radial velocity component of fluid due to centrifugal effects. The kinetic energy associated with the radial velocity component decreases near the casing, causing a pressure rise. The pressure rise initiates the flow along the axial direction both upstream (through the clearance), and downstream (backflow in the wall proximity). The backflow causes the vortex creation. However, for the higher pressure difference, the mass flow rate through the gap is larger, while the backflow decreases and finally disappears. Thus, when the inlet pressure is high the vortex does not exist (Figure 10).

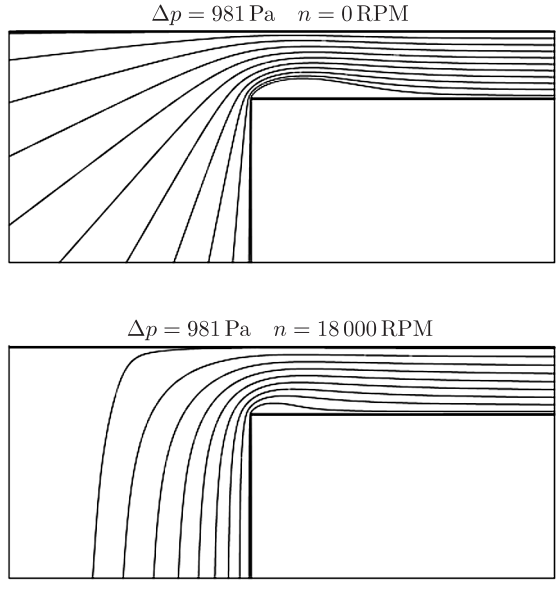

Figure 10. Streamlines entering the gap for $\Delta p = 981\,\mathrm{Pa}$ and rotational velocity 0 RPM and 18 000 RPM

Moreover, the disk has to induce sufficiently high radial velocity of fluid; hence, the rotation velocity has to be high for the vortex to be generated. The creation of the vortex upstream of the disk is a phenomenon that does not exist in a real turbine, as the fluid flow is not blocked by the disk. The vortex influences the inflow angle at which the fluid enters the gap, which is shown in Figure 9. Therefore, the conditions are different than in an actual turbine. Thus, for future work, an improved model will be considered in order to take into account the fluid flow through the disk with the same pressure drop as the pressure drop in a turbine stage.

The flow separates at the edge of the disk at the entrance of a gap. The size of the vortex in that region is dependent on the flow distribution upstream of the gap and the rotational speed and on pressure difference. However, the impact of the rotation velocity seems to be most significant. Figure 11 shows the streamlines in a gap between the disk and the casing and Figure 12 presents the length of the separation bubble to gap height ratio with respect to the u/w parameter.

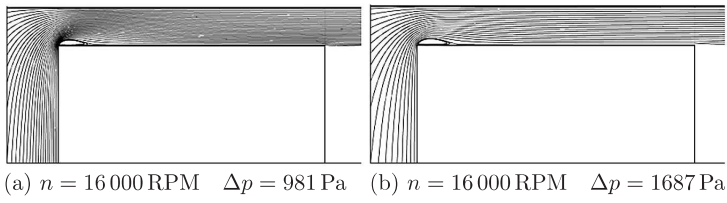

(a) $n = 16\,000$ RPM $\Delta p = 981$ Pa (b) $n = 16\,000$ RPM $\Delta p = 1687$ Pa

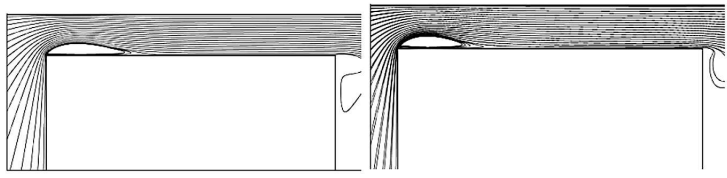

(c) $n = 0$ RPM $\Delta p = 981$ Pa (d) $n = 0$ RPM $\Delta p = 1687$ Pa

Figure 11. Streamlines in the gap for various pressures and circumferential velocities

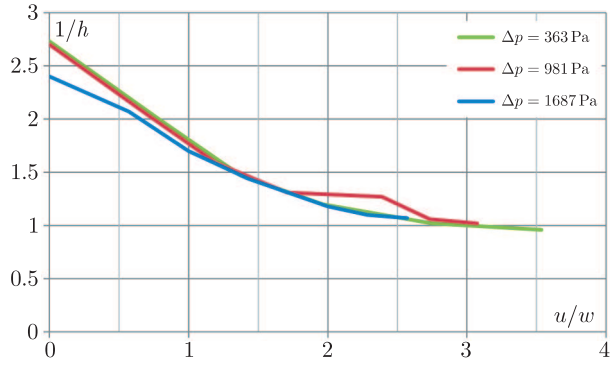

Figure 12. Separation bubble length to gap height ratio with respect to u/w, for various preside differences Δp

The length of the separation bubble is the distance measured between the disk edge and the point in the proximity of the disk cylindrical surface on which the shear stress was equal to zero. It can be observed, that the separation bubble is larger when there is no rotation, and that its size does not depend heavily on the pressure difference.

An important flow feature is the velocity distribution in the gap. It enables to investigate non-uniformity of the flow parameters in the gap. Axial and circumferential velocity components and the velocity magnitude were plotted at

the three control planes. The first plane is located at the 10% of the gap length, the second and the third one at 50% and 90%, respectively. In Figure 13, axial and circumferential velocity components for the rotational speed 18 000 rpm and pressure difference 1687 Pa are shown at the following control planes in the gap. A comparison of the axial velocity profiles for 0 RPM and 18 000 RPM and pressure difference 1687 Pa is shown in Figure 14.

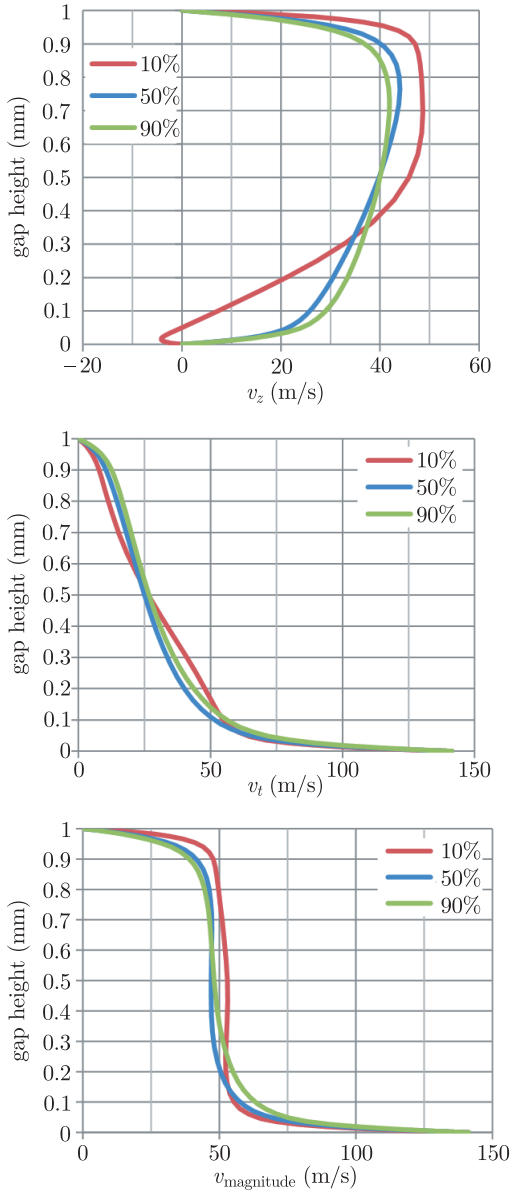

Figure 13. Axial velocity, rotational velocity and velocity magnitude in a gap at 10%, 50% and 90% of gap length

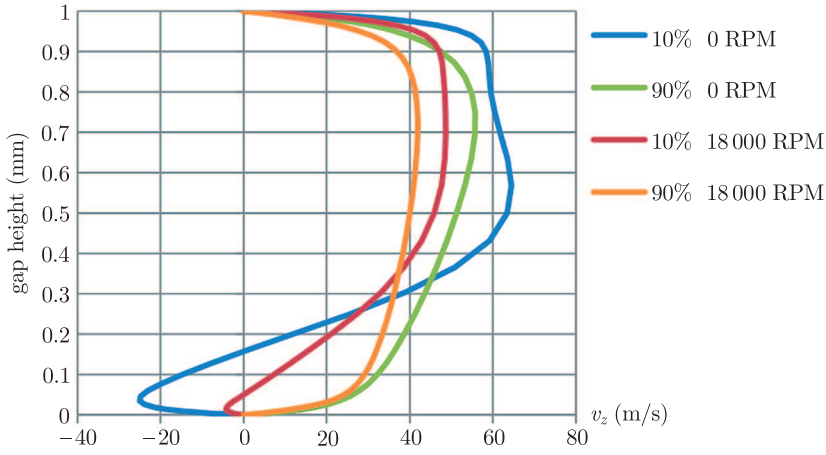

Figure 14. Comparison of axial velocity profiles in a gap at 10% and 90% of gap length

Aforementioned boundary layer separation at the gap inlet can be observed on the plots (Figures 13, 14). One has to keep in mind that the results are obtained within a framework of axisymmetric model, so the comparison can be done on the basis of two-dimensional picture, only. In meridional plane the separation size can be estimated by the axial velocity component, so the negative value indicates the range of the separation zone. The separation bubble size is larger in the case without rotation. Due to the rotation the velocity increases near the wall and the shear stresses increase, then the separation decreases. Such effect requires further three dimensional investigations, because within separation zone the vortex is spread in circumferential direction. Farther downstream in the gap, the axial velocity non-uniformity distribution decreases in both cases, but the mean value is lower for the case with rotation. The effect of rising rotating speed on the decreasing mass flow in the gap was already shown above.

6. Summary and further study

The impact of the pressure difference and the rotational velocity on the flow through the rotating disk was investigated with the focus on the mass flow through the clearance between the disk and the casing. The numerical calculations were performed and validated using experimental data. The study showed that disk rotation may significantly reduce the mass flow through the gap.

Furthermore, the research revealed the vortex development upstream of the disk. The source of vortex is the rotational velocity of the disk, causing the backflow. If the pressure difference is high enough, the backflow fades and the vortex disappears. However, this phenomenon will not be present in this form in an actual shrouded turbine.

Moreover, the separation bubble is created at the edge of the disk. The separation size depends both on the rotational velocity and the pressure difference, although the impact of the latter is not significant. Controlling the fluid behavior

at the gap inlet, especially the edge of the disk, is important for reduction of the mass flow rate through the clearance.

The model described in the paper will be used as a reference for future work focused on the mass flow rate reduction through the gap between the shrouded turbine blade and the casing. Further research includes examining numerically various flow control techniques on the rotating disk in order to reduce the mass flow through the gap. Afterwards the most efficient solutions will be implemented in the numerical model of an actual shrouded turbine stage and investigated.

Investigations of the simple model of a flow through a gap between the rotating disk and the casing help to establish the basis for the aforementioned future work and identify the possible problems with this approach. In the model the only way for the fluid to get downstream is the gap, whereas in the turbine it can travel through the blade passage. It influences the creation of a vortex upstream of the disk which enforces the changes of the inflow angle at which the fluid enters the gap. One of the solutions to that problem might be to model the pressure drop artificially (*i.e.* by introducing porosity) in the disk as in the blade passage of the turbine cascade.

Acknowledgements

This research was supported by CI TASK and in part by PL-Grid Infrastructure.

References

[1] Puzyrewski R and Jakubek A 1989 *Prace Instytutu Maszyn Przepływowych* **89**
[2] Puzyrewski R and Jakubek A 1991 *Prace Instytutu Maszyn Przepływowych* **93**
[3] Booth T C, Dodge P R and Hepworth H K 1982 *ASME J. Turbomachinery* **104** 154
[4] Hofer T, Legrand M, Pons L and Arts T 2009 *ASME Turbo Expo 2009: Power for Land, Sea, and Air*, Turbomachinery, Parts A and B, Orlando, Florida, USA, **7**
[5] Kanjirakkad V *et al.* 2008 *ASME J. Turbomachinery* **130** (1)
[6] Pfau A, Trieber M, Sell M and Gymrathy G 2000 *ASME Paper No. 2000-GT-0481*
[7] Wallis A M, Denton J D and Demargne A A J 2000 *ASME Paper No. 2000-GT-0475*
[8] Lehmann K, Thomas R, Hodson H and Stefanis V *ASME Turbo Expo 2009: Power for Land, Sea, and Air*, Heat Transfer, Parts A and B, Orlando, Florida, USA, **3**
[9] Stephens J 2009 *Control of the tip-gap flow of a low pressure turbine blade in a linear cascade, PhD thesis*, University of Notre Dame
[10] Spalart P R and Allmaras S R 1992 *AIAA Paper 92–0439*